The Molecular and Functional Interaction between ICln and HSPC038 Proteins Modulates the Regulation of Cell Volume*[S]

Silvia Dossena[‡1], **Rosaria Gandini**[§¶], **Grazia Tamma**[‖], **Valeria Vezzoli**[‡**2], **Charity Nofziger**[‡3], **Margherita Tamplenizza**[‡**], **Elisabetta Salvioni**[‡**], **Emanuele Bernardinelli**[‡], **Giuliano Meyer**[**], **Giovanna Valenti**[‖], **Magnus Wolf-Watz**[‡‡4], **Johannes Fürst**[§], and **Markus Paulmichl**[‡5]

From the [‡]*Institute of Pharmacology and Toxicology, Paracelsus Medical University, A-5020 Salzburg, Austria, the* [§]*Department of Physiology and Medical Physics, Innsbruck Medical University, A-6020 Innsbruck, Austria, the* [¶]*Department of Medical Biochemistry and Biophysics, Karolinska Institutet, SE-171 77 Stockholm, Sweden, the* [‖]*Department of General and Environmental Physiology, University of Bari, I-70125 Bari, Italy, the* [**]*Department of Biomolecular Sciences and Biotechnology, University of Milan, I-20133 Milan, Italy, and the* [‡‡]*Department of Chemistry, Chemical Biological Center, Umeå University, SE-90187 Umeå, Sweden*

Background: The operon structure of the *C. elegans* genome was used to identify functional interaction partners for the chloride channel ICln.
Results: Human ICln and HSPC038 functionally interact, and this interaction between the two proteins was also identified on a molecular level.
Conclusion: The functional interaction between ICln and HSPC038 modulates the regulation of the cellular volume.
Significance: The operon structure of the *C. elegans* genome can be used to identify unknown interaction partners including those of membrane proteins, and the summarized experiments provide further insight into the interactome of the connector hub ICln.

Identifying functional partners for protein/protein interactions can be a difficult challenge. We proposed the use of the operon structure of the *Caenorhabditis elegans* genome as a "new gene-finding tool" (Eichmüller, S., Vezzoli, V., Bazzini, C., Ritter, M., Fürst, J., Jakab, M., Ravasio, A., Chwatal, S., Dossena, S., Bottà, G., Meyer, G., Maier, B., Valenti, G., Lang, F., and Paulmichl, M. (2004) *J. Biol. Chem.* 279, 7136–7146) that could be functionally translated to the human system. Here we show the validity of this approach by studying the predicted functional interaction between ICln and HSPC038. In *C. elegans*, the gene encoding for the ICln homolog (*icln-1*) is embedded in an operon with two other genes, *Nx* (the human homolog of *Nx* is *HSPC038*) and *Ny*. ICln is a highly conserved, ubiquitously expressed multifunctional protein that plays a critical role in the regulatory volume decrease after cell swelling. Following hypotonic stress, ICln translocates from the cytosol to the plasma membrane, where it has been proposed to participate in the activation of the swelling-induced chloride current (ICl_{swell}). Here we show that the interaction between human ICln and HSPC038 plays a role in volume regulation after cell swelling and that HSPC038 acts as an escort, directing ICln to the cell membrane

after cell swelling and facilitating the activation of ICl_{swell}. Assessment of the NMR structure of HSPC038 showed the presence of a zinc finger motif. Moreover, NMR and additional biochemical techniques enabled us to identify the putative ICln/HSPC038 interacting sites, thereby explaining the functional interaction of both proteins on a molecular level.

ICln (nucleotide-sensitive chloride current-inducing protein) is a highly conserved, ubiquitously expressed protein cloned from an epithelial canine cell line (1). A variety of studies have identified ICln as an important player in regulatory volume decrease, the process that enables a cell to regain its original volume after swelling (2–4). Overexpression of ICln in *Xenopus laevis* oocytes (1) or in mammalian cells (5, 6) is followed by the up-regulation of chloride currents resembling those elicited by cell swelling (ICl_{swell})[6] (2, 7, 8). Furthermore, ICln-specific antibodies (9) or antisense oligodeoxynucleotides (10, 11) leading to a specific knockdown of ICln protein expression impair regulatory volume decrease in native cells. ICln is water-soluble, and in isotonic conditions the majority of the protein is located within the cytosol, whereas only a small fraction is associated with the cell membrane; nevertheless, ICln transposes from the cytosol to the cell membrane in hypotonic conditions (12–16). These studies suggest that ICln could be a molecular entity or part of the molecular arrangement determining ICl_{swell}. This hypothesis was challenged by others (17,

[6] The abbreviations used are: ICl_{swell}, swelling-activated chloride current; ECFP, enhanced cyan fluorescent protein; EYFP, enhanced yellow fluorescent protein; EGFP, enhanced green fluorescent protein; FKBP, FK506-binding protein; IRES, internal ribosome entry site; MOPS, 3-(*N*-morpholino)-propanesulfonic acid; HSQC, heteronuclear single quantum coherence; ANOVA, analysis of variance; FRAP, FKB12/rapamycin-associated protein; FRB, FKBP12/rapamycin-binding.

18); however, it is further supported because (i) purified ICln can induce ion channel activity following insertion into artificial lipid bilayers from aqueous solutions (5, 19–22), and (ii) the ion permeability observed in the presence of purified ICln protein in the extracellular solution of NIH 3T3 fibroblasts (15) and Sf9 insect cells (22) is increased. Detailed studies revealed additional functions of ICln in addition to its role in regulatory volume decrease, *i.e.* regulation of cellular morphology (23), platelet activation (24), angiogenesis (25), cell migration (26), and RNA processing (27). The role of ICln in the different functional modules was recognized either by observing a special phenotype (*i.e.* ion currents across the membrane) or by identifying its specific interactome using biochemical methods (28). So far, a variety of proteins within different cellular compartments have been identified to interact with ICln (28). For this, different "tools" were used to screen for partner proteins, *i.e.* yeast two-hybrid system, coimmunoprecipitation, affinity assays (28), and FRET (16). Because of the lack of more "rational" tools to identify functional protein partners, we set out to utilize the operon structure of the *Caenorhabditis elegans* genome to prospectively predict functionally interacting protein partners (29). We successfully used this approach for the first time and identified two possible protein partners of ICln (*icln-1*), *i.e.* Nx (*CO1F6.9*) and Ny (*lpl-1*) (5, 28–30). The human homolog of Nx is HSPC038, a small (molecular mass = 8498 Da), basic (pI = 10.02), hydrophilic protein whose function was unknown. We observed that as a consequence of coreconstituting Nx together with the IClnN2 splice variant in artificial lipid membranes, the current induced by IClnN2 was no longer voltage-sensitive, thereby revealing a functional interaction between the two *C. elegans* proteins (5). Nx and its human homolog HSPC038 have a similar amino acid sequence (29). However, in contrast to the nematode system, the human *ICln* (*CLNS1A*, chromosome 11, position 11q13.5) and *HSPC038* (chromosome 8, position 8q22.3) genes are not in close genomic proximity to each other, and no data in the literature suggested an interaction between the corresponding proteins. Nevertheless, as our data show, both human gene products establish a molecular interaction *in vivo* similarly to the *C. elegans* counterparts. These findings underscore the use of the operon structure of the nematode genome as an extremely powerful tool for the identification of partner proteins, which can be successfully translated to the human system.

EXPERIMENTAL PROCEDURES

Cloning Procedures and Plasmid Constructs—The ORFs of full-length HSPC038 and ICln were amplified by PCR using standard protocols. The PCR products were cloned in frame into the mammalian expression vectors pECFPC1, pEYFPC1, pECFPN1, or pEYFPN1 (Clontech) to produce fusion proteins suitable for FRET experiments.

For electrophysiology experiments, HSPC038 and ICln ORFs were cloned into the bicistronic mammalian expression vector pIRES2-EGFP (Clontech). Control experiments were conducted in cells transfected with the pIRES2-EGFP-EGFP vector, where an additional EGFP coding sequence was cloned into the pIRES2-EGFP (Clontech) expression vector. Consequently, a single control vector contains two EGFP coding

sequences (one in the multiple cloning site and one downstream of the IRES sequence). For electrophysiology experiments where HSPC038-ICln dimerization was drug-induced, the HSPC038 ORF was subcloned into the pC4-RHE vector (ARGENT™-regulated heterodimerization kit, version 2.0; Ariad Pharmaceuticals, Cambridge, MA; now iDimerize, Clontech). Then the HSPC038-FRB or FRB-HSPC038 coding sequences were subcloned into the pIRES2dsREDexpress vector (Clontech). The final constructs allowed for the coexpression of the dsREDexpress protein with either (i) HSPC038 with the FRB domain fused to the C terminus (HSPC038-FRB) or (ii) HSPC038 with the FRB domain fused to the N terminus (FRB-HSPC038). A similar procedure was adopted for ICln: the ICln ORF was subcloned into the pC4EN-F1 and pC4M-F2E vectors and then into pIRES2-EGFP. The final constructs allowed for the coexpression of the EGFP protein with either (i) ICln with a single FKBP domain fused to the C terminus (ICln-FKBP) or (ii) ICln with two FKBP domains fused to the C terminus and a myristoylation sequence fused to the N terminus (myr-ICln-FKBP-FKBP). The myristoylation sequence enabled the fusion protein to be targeted to the plasma membrane. The use of vectors bearing the internal ribosome entry site (IRES) allows for the simultaneous expression of two individual proteins (HSPC038 or ICln and EGFP or the dsRedExpress protein) from a single bicistronic mRNA without the production of fusion proteins (31). Therefore, because EGFP or dsRedExpress expression occurs only if preceded by HSPC038 or ICln expression, the single transfected cells can be individuated optically by detecting the fluorescent light emitted by EGFP (excitation maximum, 488 nm; emission maximum, 507 nm) or dsRedExpress (excitation maximum, 557 nm; emission maximum, 579 nm). HSPC038 was also cloned into the mammalian expression plasmid pFLAG-CMV4 (Sigma) for overexpression of the N-terminally FLAG (DYKDDDDK)-tagged protein.

For protein purification, the ORFs of ICln and its deletion mutants (19, 32), as well as HSPC038, were cloned in frame with a hexahistidine tag (coding for MHHHHHHLE) into the bacterial expression vector pET3-His (33), allowing for the expression of N-terminal His$_6$-tagged proteins in *Escherichia coli* strains. All of the plasmid inserts were sequenced prior to use in experiments (Microsynth AG).

Cell Culture and Transient Transfection—Standard procedures were utilized for culturing the respective cells and for transfection. A detailed description of the procedures is given in the supplemental materials.

Patch Clamp Recordings—HEK293 Phoenix cells were transfected with the bicistronic mammalian expression vector pIRES2-EGFP coding for EGFP only (controls; pIRES2-EGFP-EGFP) or EGFP and ICln (or EGFP and HSPC038) as separate proteins. Single cells expressing EGFP were selected by fluorescence microscopy and voltage-clamped using the whole cell patch clamp technique. The resistance of the glass pipettes was 3–8 MΩ when filled with the pipette solution (125 mM CsCl, 5 mM MgCl$_2$, 11 mM EGTA, 50 mM raffinose, 2 mM ATP, 10 mM HEPES, pH 7.2 (adjusted with CsOH)). The hypertonic bath solution was composed of 125 mM NaCl, 2.5 mM CaCl$_2$, 2.5 mM MgCl$_2$, 10 mM HEPES, 100 mM mannitol, pH 7.4 (adjusted with NaOH). Fast exchange of the hypertonic bath solution with a hypotonic bath

solution (125 mM NaCl, 2.5 mM CaCl$_2$, 2.5 mM MgCl$_2$, 10 mM HEPES, pH 7.4) was obtained using a perfusion system with a flow rate of 5 ml/min and a bath volume of ~300 μl. For the experiments where purified proteins were added to the pipette filling (intracellular) solution, 15 μg/ml ICln (0.57 μM), 15 μg/ml HSPC038 (1.76 μM), or equimolar amounts of ICln and HSPC038 (1.76 μM each, 46 μg/ml and 15 μg/ml, respectively; the use of equimolar amount of proteins does not imply a 1:1 stoichiometry of the putative ICln-HSPC038 complex) were used. For the control experiments, an adequate volume of the appropriate elution buffer was added to the pipette filling solution. The diffusion of substances from the pipette filling solution to the intracellular milieu was verified with 10 μg/ml fluorescent dextrans (molecular mass = 40,000 Da; Molecular Probes) after the establishment of the whole cell configuration. All of the experiments were carried out at room temperature. Additional details regarding data acquisition are given in the supplemental materials.

FRET Measurements—FRET studies were performed as described earlier (15). Briefly, the cells were double transfected with pECFP-mem (Clontech) and pEYFPN1-HSPC038 or pECFPN1-ICln and pEYFPN1-HSPC038. Transfected cells were perfused at room temperature with an isotonic solution containing 90 mM NaCl, 5 mM KCl, 2 mM CaCl$_2$, 2 mM MgCl$_2$, 5 mM glucose, 80 mM mannitol, 10 mM HEPES, pH 7.4). After recording the fluorescent signals under isotonic conditions, the cells were perfused with a hypotonic solution (90 mM NaCl, 5 mM KCl, 2 mM CaCl$_2$, 2 mM MgCl$_2$, 5 mM glucose, 10 mM HEPES, pH 7.4), and ECFP, EYFP, and FRET images were recorded after 5, 15, and 30 min following hypotonic shock. Additional details are given in the supplemental materials.

Protein Expression and Purification—All of the proteins were overexpressed as N-terminal His$_6$-tagged fusion proteins in *E. coli* BL21 (DE3) or BL21 (DE3) pLys bacteria. Bacterial cells were grown in LB medium at 37 °C until an A_{600} of 0.8. Protein overexpression was induced by adding isopropyl-1-thio-β-D-galactopyranoside to the bacterial culture to a final concentration of 0.3 mM. Bacterial cells were harvested 4 h after induction. His$_6$-tagged fusion proteins were purified using standard protocols described in detail in the supplemental materials.

Native PAGE Experiments—50 μg of purified recombinant HSPC038, 50 μg of ICln, or a mixture of the two proteins were incubated in a buffer containing 25 mM K$_2$HPO$_4$, 150 mM NaCl, 5% glycerol, pH 7.2, for 2 h at 4 °C and subsequently separated on 10% native PAGE gels.

Affinity Chromatography Experiments—Purified recombinant HSPC038 was coupled to CNBr-activated Sepharose 4B beads (Sigma) according to the manufacturer's instructions. Control beads were prepared by coupling ethanolamine instead of protein to CNBr-activated Sepharose 4B beads. Aliquots of either HSPC038-coupled resin or control beads were then incubated with purified ICln or its mutants (final concentration, 1 mg/ml) in a buffer containing 25 mM MOPS, 150 mM NaCl, pH 7.2, for 2 h at 4 °C. After extensive washing, bound ICln proteins were eluted by low pH buffer (500 mM Tris, pH 2.5), and elution fractions were neutralized by the addition of 500 mM Tris, pH 8.0, and then separated by SDS-PAGE.

NMR Spectroscopy—All of the NMR experiments were acquired at 25 °C on a Bruker DRX 600 MHz spectrometer equipped with a 5-mm triple resonance z-gradient cryoprobe. NMR data were processed and visualized using the NMRPipe software (34) and ANSIG for Windows (35). Resonance assignments of HSPC038 was accomplished with three-dimensional ^{15}N NOESY-HSQC and ^{15}N total total correlation spectroscopy-HSQC experiments from the Bruker program library. Partial backbone resonance assignments of ICln 1–159 were made based on published assignments (36). To map the interaction interfaces upon interaction between HSPC038 and ICln 1–159, two protein samples were prepared: one with ^{15}N labeled HSPC038 (0.8 mM) and unlabeled ICln 1–159 (0.9 mM), and the second with ^{15}N-labeled ICln 1–159 (1 mM) and unlabeled HSPC038 (3 mM). The chemical shift perturbations following complex formation were small, and assignments of the complexes were based on the assignments of the free proteins. Perturbations in resonance frequency ($\Delta \nu$) resulting from complex formation was analyzed using Equation 1,

$$\Delta \nu = \sqrt{(\Delta \nu^H)^2 + (\Delta \nu^N)^2} \qquad \text{(Eq. 1)}$$

where $\Delta \nu^H$ and $\Delta \nu^N$ are perturbations in ^{1}H and ^{15}N resonance frequency, respectively.

Homology Modeling of the HSPC038 Zinc Finger Motif—A homology model of the zinc finger motif of HSPC038 was generated with Swiss model (37, 38) using the first zinc finger motif of conformer number one in Protein Data Bank code 2GHF as the template.

RNA Interference—siRNAs for knocking down the expression of HSPC038 (core sequence: 5′-GAA ACA AGG ACA UGA CCA A-3′) were designed with the siRNA Design Tool of Microsynth CH. HEK293 Phoenix cells seeded into Ø 30-mm Petri dishes were transfected with 180 pmol of siRNAs and 12 μl of Metafectene SI (Biontex) following the manufacturer's instruction. Control cells were transfected with the following negative control siRNA (Microsynth CH): 5′-AGGUAGU-GUAAUCGCCUUG-3′. Functional (patch clamp) or expression (semiquantitative reverse transcription-PCR) assays were performed 48–56 h after transfection.

Semiquantitative Reverse Transcription-PCR—Extraction of total RNA was performed with the All Prep DNA/RNA mini kit (Qiagen). 1 μg of total RNA was used for the reverse transcription reaction with the QuantiTect® reverse transcription kit for cDNA synthesis with integrated removal of genomic DNA contamination (Qiagen). For detecting the *HSPC038* transcript, the following primers were used: forward, 5′-CGT GGA CAG CAG AAG ATT CAG-3′; and reverse, 5′-AGT GGA GCT TTA GGG TGC TTG-3′. The *HSPC038* signal was normalized to the β-actin signal, detected by using the following primers: forward, 5′-GGCATGGGTCAGAAGGATTC-3′; and reverse, 5′-AGAG-GCGTACAGGGATAGCAC-3′. These primers span an intron-exon boundary and would disclose an eventual contamination from genomic DNA as a band at 700 bp, which was not detected (see Fig. 8*a*). Densitometric analysis was done with the ImageJ 1.38x program.

Western Blot—Standard protocols described in detail in the supplemental materials were used.

Salts, Chemicals, and Drugs—All salts and chemicals used were of "*pro analysis*" grade.
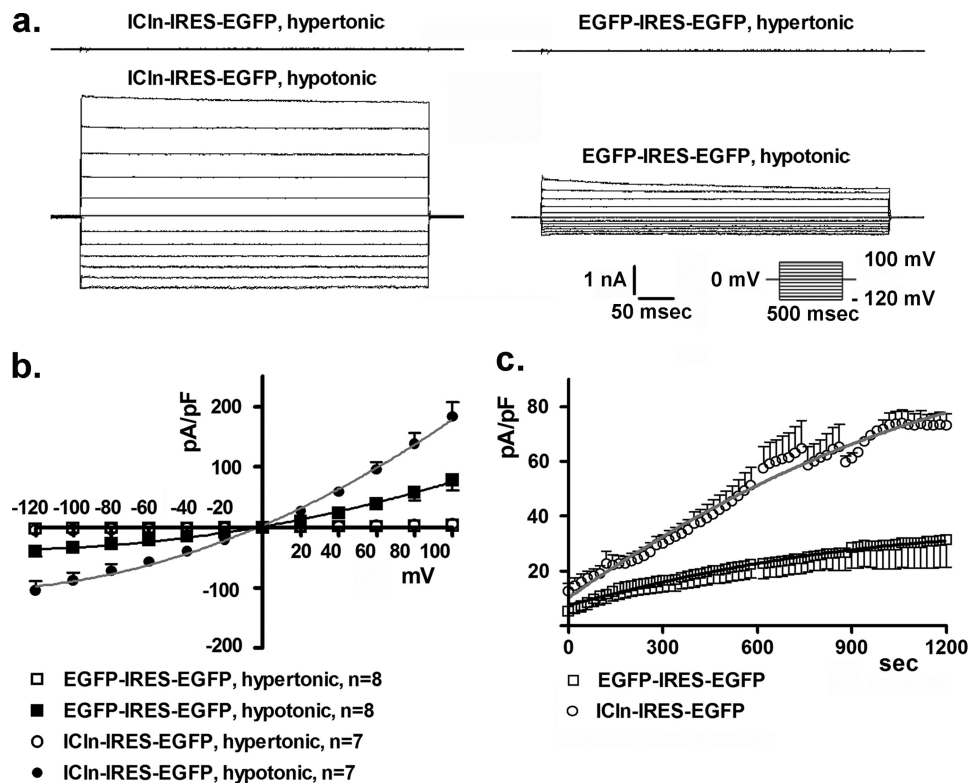
FIGURE 1. **ICln overexpression increases ICl$_{swell}$.** ICl$_{swell}$ activation was monitored in HEK293 Phoenix overexpressing both ICln and the transfection marker EGFP as separate proteins. Experiments were done in whole cell configuration. *a*, original recordings obtained in hypertonic (*upper traces*) or hypotonic conditions (*lower traces*) in ICln transfected (ICln-IRES-EGFP) or control (EGFP-IRES-EGFP) cells with voltage increments of 20 mV from -120 to $+100$ mV applied at a holding potential of 0 mV. *b* and *c*, the current density-to-voltage relationship measured 10 min following hypotonic shock (*b*) and the current density-to-time relationship (*c*) show up-regulation of ICl$_{swell}$. The data were fitted with second order polynomials following application of the extra sum of squares F test (EGFP-IRES-EGFP *versus* ICln-IRES-EGFP: $p < 0.0001$).

Statistical Analysis—All of the data are expressed as arithmetic means $\pm$ S.E. For statistical analysis, GraphPad Prism software (version 4.00 for Windows; GraphPad Software, San Diego, CA) was used. Significant differences between means were tested by paired Student's t test or ANOVA. Statistically significant differences were assumed at $p < 0.05$ (*, $p < 0.05$; **, $p < 0.01$; ***, $p < 0.001$); n corresponds to the number of independent experiments. The current density-to-time and current density-to-voltage relationships were fitted with second order polynomials ($Y = A + BX + CX^2$). For detecting significant differences between those data, the extra sum of squares F test was applied. Statistically significant differences were assumed at $p < 0.01$.

RESULTS

ICln or HSPC038 Overexpression Activates ICl$_{swell}$—As previously described for the *C. elegans* IClnN1 (5), the expression of the human ICln isoform in HEK293 Phoenix cells also leads to an increased ICl$_{swell}$ (Fig. 1). Cells were transiently transfected with either the pIRES2-EGFP vector encoding for ICln or with the control vector pIRES2-EGFP-EGFP; for electrophysiological measurements, cells were initially kept in extracellular hypertonic solution. After the seal was realized and the whole cell configuration was obtained, ICl$_{swell}$ activation was monitored following reduction of the extracellular osmolarity by 100 mM via omission of mannitol. Hypotonic shock induced the activation of a large chloride current with the biophysical fin-

gerprints of ICl$_{swell}$ (outward rectification, slow voltage- and time-dependent inactivation at positive potentials; Fig. 1*a*) in both control and ICln-overexpressing cells. The current density-to-voltage (Fig. 1*b*) relation determined after a 10-min exposure to extracellular hypotonic solution and the current density-to-time relation (Fig. 1*c*) both showed a higher increase of ICl$_{swell}$ in ICln-overexpressing cells with respect to the control cells ($p < 0.0001$). A similar effect was observed in cells overexpressing HSPC038 (Fig. 2). The current density-to-voltage relation (Fig. 2*b*) measured at the maximal current activation and the current density-to-time relation (Fig. 2*c*) both clearly show that ICl$_{swell}$ was increased in HSPC038 transfected cells with respect to the control cells ($p < 0.0001$). It is important to mention that the described experiments were conducted on single transfected cells selected by detecting the EGFP fluorescence; the constructs used allow the simultaneous expression of the protein of interest (ICln or HSPC038) and EGFP as separate proteins in the same cell; EGFP expression can only occur if ICln or HSPC038 is also expressed.

Purified ICln and/or HSPC038 Protein Activates ICl$_{swell}$—Similar experiments were performed in which purified ICln or HSPC038 proteins were added to the pipette filling solution (after establishing whole cell configuration, the purified protein will access the intracellular space). For these experiments, nontransfected cells were used. ICl$_{swell}$ activation was elicited and measured as previously described. The current density-to-volt-
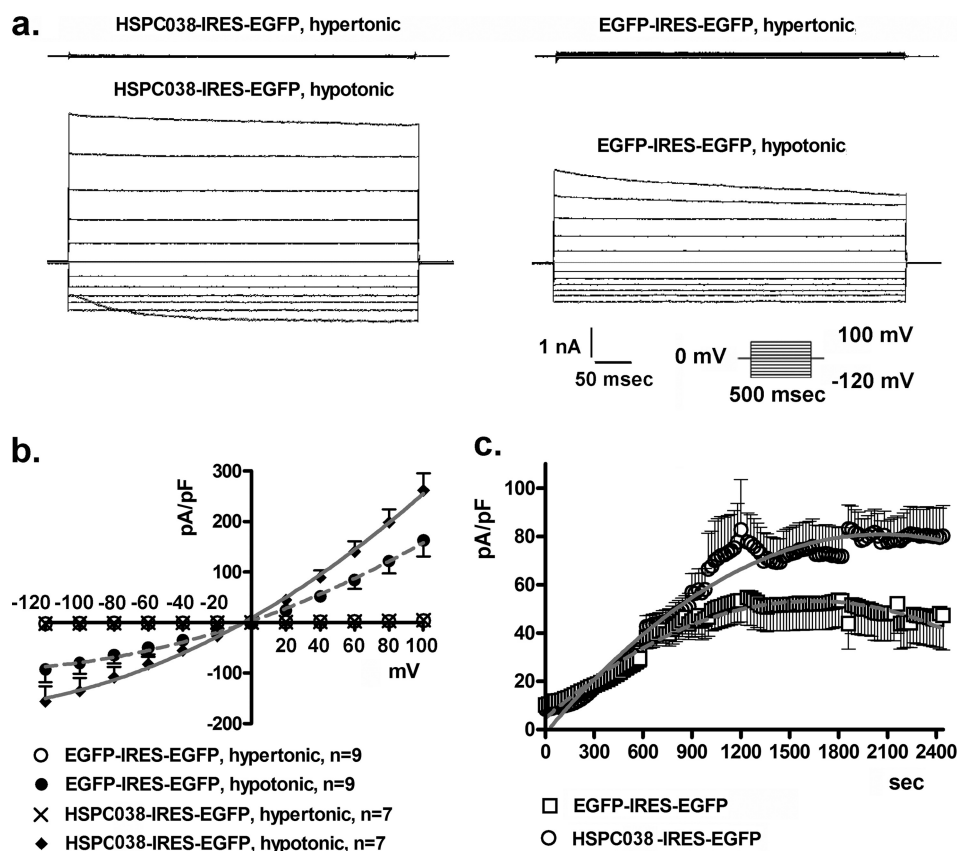
FIGURE 2. **HSPC038 overexpression increases ICl$_{swell}$.** ICl$_{swell}$ activation was monitored in HEK293 Phoenix cells overexpressing both HSPC038 and the transfection marker EGFP as separate proteins. Experiments were done in the whole cell configuration. *a*, original recordings obtained in hypertonic (*upper traces*) or hypotonic conditions (*lower traces*) in HSPC038 transfected (HSPC038-IRES-EGFP) or control (EGFP-IRES-EGFP) cells with voltage increments of 20 mV from −120 to +100 mV applied at a holding potential of 0 mV. *b* and *c*, the current density-to-voltage (*b*) and the current density-to-time relationships (*c*) showing an up-regulation of ICl$_{swell}$. The data were fitted with second order polynomials following application of the extra sum of squares F test (EGFP-IRES-EGFP *versus* HSPC038-IRES-EGFP in hypertonicity: not significant; in hypotonicity: $p < 0.0001$).

age relation was measured at the maximal current activation with either purified ICln (15 μg/ml; Fig. 3*a*) or purified HSPC038 (15 μg/ml; Fig. 3*b*). These data and the respective current density-to-time relations (Fig. 3*c*) show a clear current increase with respect to the control ($p < 0.0001$). Control experiments were done by addition of an appropriate volume of vehicle (immobilized metal ion affinity chromatography elution buffer) to the pipette solution. Patch clamp experiments were also performed in which both purified ICln and HSPC038 proteins (in an equimolar concentration of 1.76 μM each) were added to the pipette filling solution (native cells were used). ICl$_{swell}$ activation was elicited and measured as already described. The current density-to-voltage relation determined 15 min after the establishment of hypotonic conditions (Fig. 4*a*), and the respective current density-to-time relations (Fig. 4*b*) clearly show that in the presence of both ICln and HSPC038 in the pipette solution, ICl$_{swell}$ activation was higher compared with the addition of ICln alone ($p < 0.0001$).

HSPC038 Interacts with ICln in Vitro—To assess whether HSPC038 can interact with ICln and to identify the potential ICln binding site for HSPC038, native PAGE experiments were performed (Fig. 5, *a–d*). Purified recombinant ICln or ICln truncation mutants were incubated with purified recombinant HSPC038 (see "Experimental Procedures") and separated by

native PAGE. HSPC038 is a basic protein that migrates toward the cathode and does not enter the gel matrix; it will only enter the gel if it is bound to a negatively charged protein (for example, ICln). Thus, a band of a higher molecular mass with respect to ICln can appear only when an interaction between the two proteins occurs and therefore indicates the presence of a complex. A complex was detected for full-length ICln (ICln 1–235) and ICln 1–159, (Fig. 5, *a* and *b*), but not for ICln 158–235 (Fig. 5*d*). HSPC038 bound only weakly to ICln 1–134 (Fig. 5*c*). These results indicate that the main binding site(s) for HSPC038 on ICln are located between residues 1 and 159. The interaction between HSPC038 and ICln or its truncation mutants was also studied by affinity chromatography (Fig. 5, *e–h*). Purified HSPC038 was coupled to CNBr-activated Sepharose 4B beads (see "Experimental Procedures") and then incubated with ICln or its truncation mutants; eluates were then subjected to SDS-PAGE. HSPC038 interacted with full-length ICln (ICln 1–235) and ICln 1–159 and showed a faint interaction with ICln 1–134 (Fig. 5, *e–g*) but not with ICln 158–235 (Fig. 5*h*). The weak interaction of HSPC038 for ICln 1–134 compared with the strong interaction for ICln 1–159 suggests that the region 135–159 is important for complex formation, although the main interacting sites are located upstream. ICln 116–235 still shows a good interaction with HSPC038, whereas ICln 135–235 only shows a weak interaction (supplemental Fig. S1). Because ICln

FIGURE 3. **Purified ICln *or* HSPC038 increase ICl$_{swell}$.** ICl$_{swell}$ activation was monitored in HEK293 Phoenix cells in the whole cell patch clamp configuration. The current density-to-voltage relationships of ICl$_{swell}$ (at maximal activation) measured with 15 μg/ml of purified ICln (0.57 μM) (*a*) or HSPC038 (1.76 μM) (*b*) in the pipette filling (intracellular) solution and the respective current density-to-time graph (*c*) are shown. The data were fitted with second order polynomials following application of the extra sum of squares F test (ICln *versus* control or HSPC038 *versus* control: *p* < 0.0001).
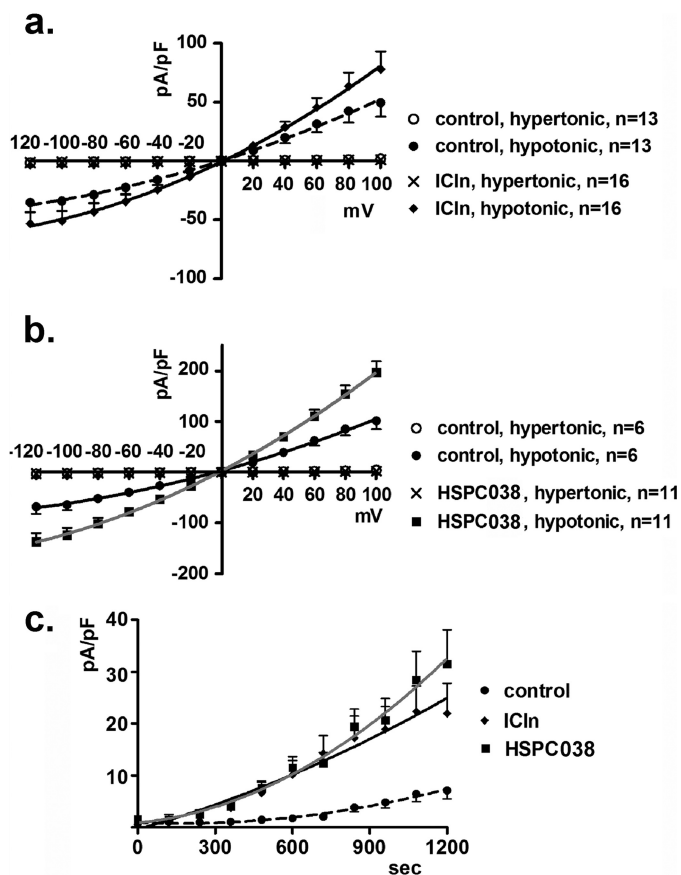
FIGURE 4. **Purified ICln and HSPC038 increase ICl$_{swell}$.** ICl$_{swell}$ activation was monitored in HEK293 Phoenix cells in the whole cell patch clamp configuration. The current density-to voltage relationship (15 min after hypotonic shock) (*a*) and the respective current density-to-time graph (*b*) of ICl$_{swell}$ were measured with 1.76 μM of purified ICln alone or with an equimolar (1.76 μM each) amount of both ICln and HSPC038 proteins in the pipette filling solution. The data were fitted with second order polynomials following application of the extra sum of squares F test (ICln and HSPC038 *versus* ICln alone: *p* < 0.0001).

158–235 does not show any interaction, we conclude that the amino acids 135–159 have a role in stabilizing the ICln-HSPC038 complex.

Hypotonic Shock Induces HSPC038 Translocation toward the Cell Membrane in Spatial Proximity to ICln—Knowing that (i) the ICln and HSPC038 homologs of *C. elegans* are able to establish a functional interaction *in vitro* (5), (ii) human ICln and HSPC038 establish a molecular interaction *in vitro* (see above) and *in vivo* under isotonic conditions (29), and (iii) ICln translocates to the cell membrane after hypotonic shock (12–16), we asked whether (i) HSPC038 also translocates to the cell membrane following hypotonic shock and (ii) the interaction between ICln and HSPC038 is influenced by hypotonicity. For this reason, we initiated FRET experiments in principal collecting duct M1 cells transfected with HSPC038 and a membrane label (pECFP-mem; Fig. 6, *a* and *b*) or ICln and HSPC038 (Fig. 6, *c* and *d*) cloned in the suitable vectors for FRET (15). Fig. 6*a* shows that the FRET signal between HSPC038 and the membrane label pECFP-mem significantly increased after hypotonic shock (the data are normalized for the FRET emission determined in isotonic conditions; the normalized netFRET was 1.00 ± 0.03 in isotonic conditions, 1.79 ± 0.11 5 min after hypotonic conditions were established, 1.88 ± 0.12 after 15
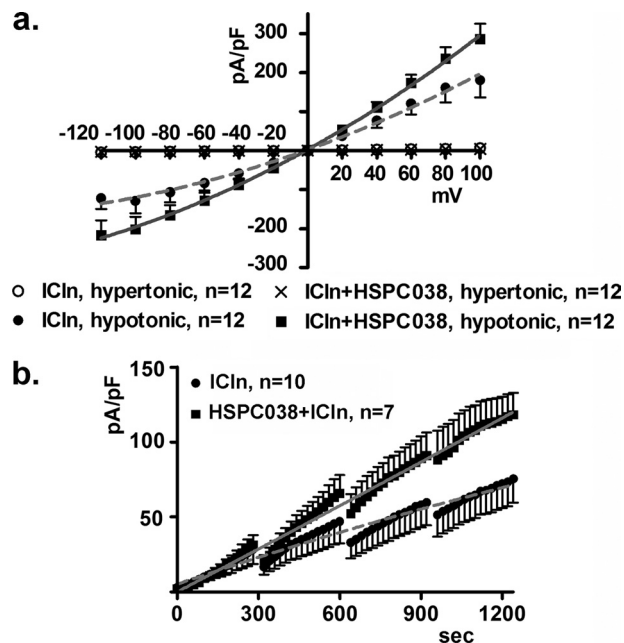
min, and 1.78 ± 0.19 after 30 min, *n* = 28; *p* < 0.05; Fig. 6*b*). These results indicate a close proximity between HSPC038 and the membrane label in hypotonic conditions, and are therefore suggestive of a translocation of HSPC038 toward the plasma membrane after hypotonic shock. Fig. 6*c* shows that the FRET signal between HSPC038 and ICln significantly increased after hypotonic shock; the normalized netFRET was: 1.00 ± 0.03 in isotonic conditions, 1.31 ± 0.07 5 min after hypotonic conditions were established, 1.44 ± 0.12 after 15 min and 1.49 ± 0.09 after 30 min, *n* = 27 (*p* < 0.05; Fig. 6*d*). These results suggest that the interaction between HSPC038 and ICln significantly increases after hypotonic shock. The presence of the fluorescent tags used for the FRET experiments (small hydrophilic proteins) do not influence the subcellular localization and redistribution of ICln after hypotonic shock (13–15).

HSPC038 Improves the Translocation of ICln to the Cell Membrane after Hypotonic Shock—To assess whether ICln abundance at the membrane level is modified by HSPC038, Western blots were performed in total membrane protein extracts from cells transfected with HSPC038 (FLAG HSPC038) or with the empty vector (FLAG empty) in isotonic conditions (0 min) or after 5, 15, and 30 min of hypotonic shock (supplemental Fig. S2*a*). Densitometry of the endogenous ICln signal normalized to the Na$^+$/K$^+$-ATPase signal shows that, following hypotonic shock, the amount of ICln in total cell membranes was significantly higher in HSPC038 transfected cells compared with mock transfected (FLAG empty) controls (supplemental Fig. S2*b*; FLAG HSPC038: 0.15 ± 0.02 *n* = 19 (isotonic conditions, 0 min); 0.36 ± 0.07, *n* = 20 (5 min after hypotonic shock); 0.29 ± 0,07, *n* = 20 (15 min after hypotonic
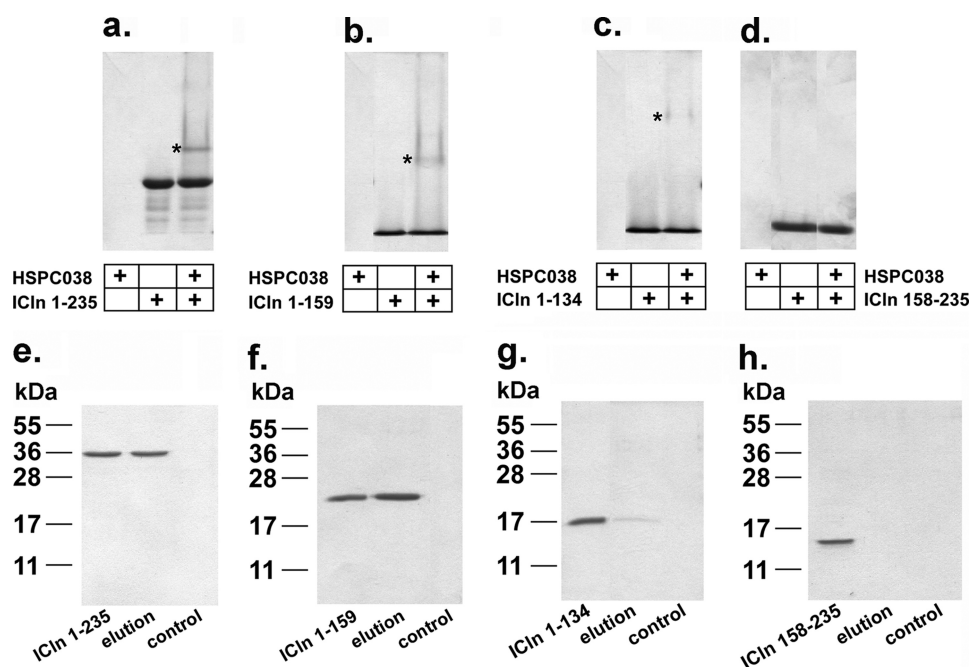
FIGURE 5. **Molecular interaction between ICln and HSPC038.** For each panel, HSPC038, ICln and its truncation mutants or a mix of HSPC038 and ICln or its truncation mutants separated by native PAGE are shown in the first, second, and third lanes, respectively. A band of higher molecular mass (*asterisk*), indicating the presence of a complex between ICln and HSPC038, was detected for full-length ICln (ICln 1–235, $n = 5$) (*a*), ICln 1–159 ($n = 5$) (*b*), and ICln 1–134 ($n = 4$) (*c*), but not for ICln 158–235 ($n = 2$) (*d*). Affinity chromatography eluates separated by SDS-PAGE of ICln 1–235 (*e*), ICln 1–159 (*f*), ICln 1–134 (*g*), and ICln 158–235 (*h*). For each panel, *first lane*, input; *second lane*, elution; and *third lane*, control (*i.e.* the elution fraction from beads with no HSPC038 bound to the resin). The presence of a band in the elution fraction indicates that full-length ICln or its truncation mutants interacted with HSPC038. No interaction was detected for ICln 158–235 (*h*); $2 \leq n \leq 4$.
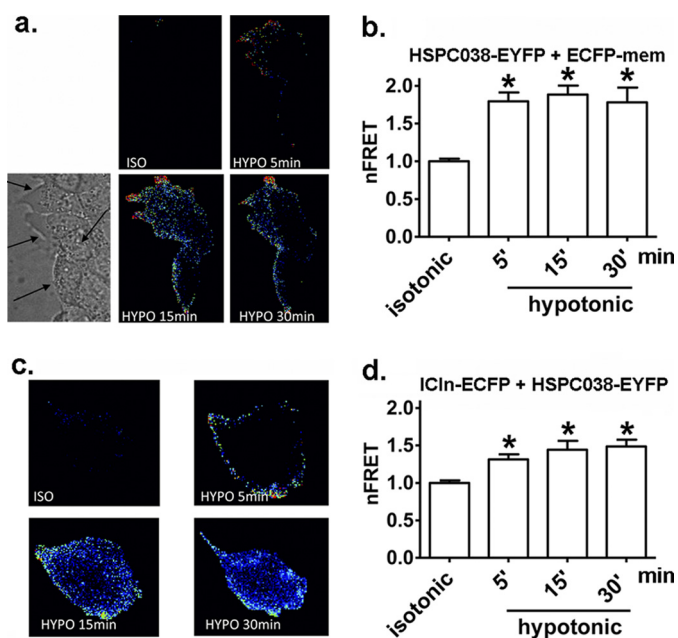

FIGURE 6. **FRET between HSPC038 and the plasma membrane and between HSPC038 and ICln following hypotonic shock.** *a*, FRET signal in principal collecting duct M1 cells transfected with the HSPC038-EYFP fusion protein and a membrane label (ECFP-mem) in isotonic conditions and after 5, 15, and 30 min of hypotonic shock; the *lower left panel* shows the transmission image of the same cells as indicated by the *arrows*. *b*, netFRET normalized to the value measured in isotonic conditions (netFRET, *nFRET*); summary of experiments shown in *a*; $n = 28$. *, $p < 0.05$ *versus* isotonic. The data were statistically analyzed by a one-way ANOVA test followed by Tukey's multiple comparison test. *c*, FRET signal in cells transfected with the HSPC038-EYFP and ICln-ECFP fusion proteins in isotonic conditions and after 5, 15, and 30 min of hypotonic shock. *d*, netFRET; summary of the experiments shown in *c*; $n = 27$. *, $p < 0.05$ *versus* isotonic, Student's *t* test. *n* indicates the number of cells.

shock); 0.38 ± 0.09, $n = 18$ (30 min after hypotonic shock); FLAG empty: 0.13 ± 0.03 $n = 20$ (isotonic conditions, 0 min); 0.11 ± 0.02, $n = 19$ (5 min after hypotonic shock); 0.15 ± 0.03, $n = 20$ (15 min after hypotonic shock); and 0.12 ± 0.02, $n = 20$ (30 min after hypotonic shock); $p < 0.001$, two-way ANOVA).

HSPC038 Does Not Modify ICln Expression—To test whether or not the increase in ICl_{swell} measured after exogenous HSPC038 expression is induced by an increased expression of endogenous ICln, Western blots in cells transfected with HSPC038 (pIRES2-HSPC038-EGFP) or with control vectors (pIRES2-EGFP-EGFP and pIRES2-EGFP) were performed. Supplemental Fig. S3*a* shows the endogenous ICln expression in total cell lysates. Densitometry of the ICln signal normalized for the tubulin signal showed no statistical differences between the groups (supplemental Fig. S3*b*; pIRES2-HSPC038-EGFP, 1.649 ± 0.18, $n = 6$; pIRES2-EGFP-EGFP, 1.4 ± 0.1, $n = 8$; pIRES2-EGFP, 1.5 ± 0.13, $n = 8$; not significant *versus* pIRES2-HSPC038-EGFP, one-way ANOVA).

The Drug-induced HSPC038-ICln Interaction Also Activates ICl_{swell}—To gather more information regarding the effect of a putative ICln-HSPC038 interaction on ICl_{swell}, both proteins were expressed with epitopes suitable for inducing their dimerization following treatment with a "dimerizer" agent (rapalog; final concentration, 500 nM). ICln was fused with either one or two FK506-binding proteins (FKBP), whereas HSPC038 was fused to the PI3K homolog FRAP-binding domain (FRB). The FKBP fusion protein binds the rapalog, which in turn becomes a binding target for the FRB fusion protein. This system is based on the model of the immunosuppressive drug rapamycin that binds the intracellular FKBP and

a. **myr-ICln-FKBP-FKBP + FRB-HSPC038**

b. **myr-ICln-FKBP-FKBP + HSPC038 -FRB**
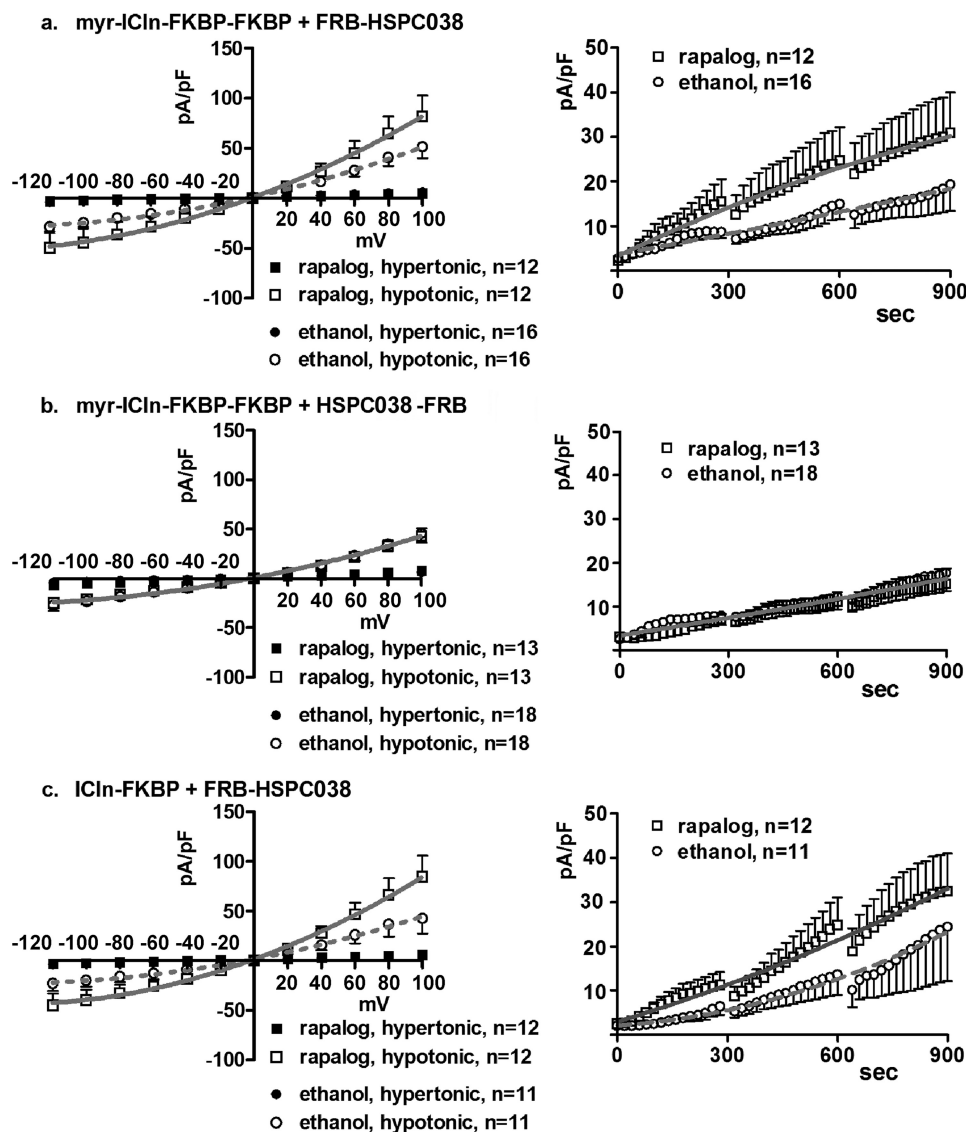

c. **ICln-FKBP + FRB-HSPC038**

FIGURE 7. **Effects of HSPC038-ICln induced dimerization on ICl$_{swell}$ activation.** ICl$_{swell}$ activation was monitored after hypotonic shock in HEK293 Phoenix cells overexpressing HSPC038, ICln, and the transfection markers as separate proteins (EGFP and dsRed). The experiments were done in the whole cell configuration; the current density-to-voltage (*left*) and the current density-to-time (*right*) relationships are shown. ICln was expressed with one (*c*) or two (*a* and *b*) FKBP epitopes fused to the C terminus, with (*a* and *b*) or without (*c*) a myristoylation signal at the N terminus; HSPC038 was expressed with one FRB epitope fused to the N terminus (*a* and *c*) or to the C terminus (*b*). FKBP and FRB epitopes are suitable for inducing the heterodimerization between the two proteins following overnight incubation with the rapalog (AP21967, 500 nM). Controls were done with an appropriate amount of vehicle (ethanol). The data were fitted with second order polynomials following application of the extra sum of squares F test (*a* and *c*: rapalog *versus* ethanol: $p < 0.0001$ in hypotonicity; in hypertonicity the current measured after incubation with rapalog is not increased with respect to the current measured after incubation with ethanol; in *b*, no statistical differences between the two conditions were detected).

FRAP targets (39, 40). However, the FKBP and rapalog used for these studies have been engineered so that they no longer recognize either endogenous target. In Fig. 7, the ICl$_{swell}$ current density-to-voltage relationships after 10 min of hypotonic shock (Fig. 7, *left panels*) and time courses (Fig. 7, *right panels*) are shown in cells expressing ICln with a myristoyl (membrane-targeting) tag fused to the N terminus and 2 FKBP domains fused to the C terminus (myr-ICln-FKBP-FKBP) or with one FKBP domain fused to the C terminus (ICln-FKBP) together with HSPC038 fused to one FRB domain located on either the N or C terminus (FRB-HSPC038 or HSPC038-FRB). The data show that following rapalog exposure, ICl$_{swell}$ activation is faster when the FRB domain is fused to the N terminus of HSPC038 ($p < 0.0001$; Fig. 7, *a* and *c*). These experiments show

that drug-induced HSPC038-ICln dimerization up-regulates ICl$_{swell}$, although the position (N or C terminus) of the FRB domain on HSPC038 seems to influence the effect on ICl$_{swell}$ activation and presumably on dimerization, because no effect on ICl$_{swell}$ was observed when the FRB domain was fused to the C terminus of HSPC038 (Fig. 7*b*).

HSPC038 Knockdown Impairs ICl$_{swell}$—As previously described by us (41) and others (6), ICln knockdown suppress ICl$_{swell}$ activation. Here we show that the knockdown of HSPC038 similarly leads to a decreased ICl$_{swell}$ (Fig. 8). HSPC038 knockdown was obtained in HEK293 Phoenix cells by using siRNAs as described under "Experimental Procedures" and verified by semiquantitative RT-PCR (Fig. 8*a*). Densitometry comparing the *HSPC038* signal with a housekeeping tran-
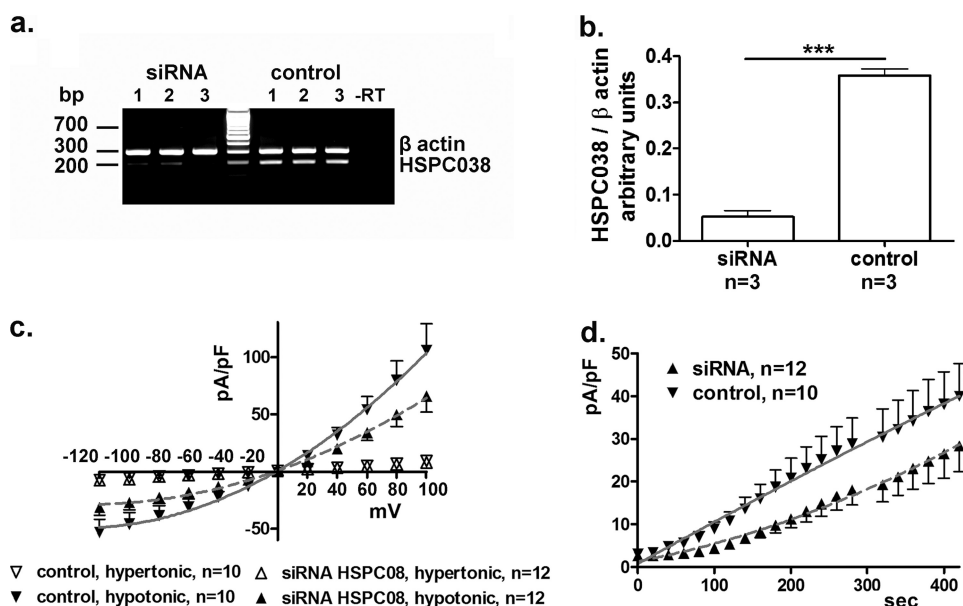
FIGURE 8. **HSPC038 knockdown impairs ICl$_{swell}$.** HSPC038 knockdown was realized by using specific siRNAs in HEK293 Phoenix cells. *a*, the levels of the transcripts of *HSPC038* and of the housekeeping gene *β-actin* were detected by RT-PCR in three independent samples of siRNA or control-siRNA (control)-treated cells. −*RT*, as a control, the PCR was conducted on a sample of total RNA that was not subjected to the reverse transcription reaction, to exclude genomic DNA contamination. *b*, densitometric analysis of the *HSPC038* signal normalized to the *β-actin* signal. ***, $p < 0.001$ between siRNA-treated cells and control siRNA-treated cells, unpaired t test. ICl$_{swell}$ activation was monitored after hypotonic shock in siRNA-treated cells or in control cells. *c* and *d*, the experiments were done in the whole cell configuration; the current density-to-voltage (*c*) and the current density-to-time (*d*) relationships are shown. The data were fitted with second order polynomials following application of the extra sum of squares F test (*c* and *d*: siRNA *versus* control: $p < 0.0001$).

script (*β-actin*) revealed that the efficiency of the *HSPC038* knockdown was ≈85% (Fig. 8*b*; $p < 0.001$, $n = 3$). ICl$_{swell}$ activation was elicited and measured as previously described in cells where the knockdown of HSPC038 was induced and compared with the current measured under control conditions. The current density-to-voltage relation measured 5 min after hypotonic shock (Fig. 8*c*) and the respective current density-to-time relation (Fig. 8*d*) show that HSPC038 knockdown induces a significant current decrease (≈40%) with respect to the control ($p < 0.0001$).

Structure of HSPC038—Our HSPC038 construct contains 85 amino acid residues including a N-terminal polyhistidine sequence for protein purification. Based on sequence alignment comparisons, HSPC038 is found to contain a C2H2 zinc finger motif comprising residues 39–62. We were able to assign the non-proline backbone NH groups of amino acids 37 through 76 with the exception of leucine 67 by using sequential NOE connectivities. A cluster of peaks exist in the random coil region of the ^{1}H-^{15}N HSQC spectrum that belong to the N-terminal sequence of HSPC038 (residues 2–36). This segment is rich in charged amino acid residues, which is a hallmark for unstructured segments in proteins. These residues could not be assigned using sequential NOE connectivities. A homology model of HSPC038 was generated based on the NMR structure of the first zinc finger motif in human ZHX1 (42) (Fig. 9*c*). The structural model was validated by analyzing sequential NOE contacts expected for the zinc finger $\beta\beta\alpha$ topology (data not shown).

Interaction Interfaces from NMR Spectroscopy—NMR chemical shifts represent a sensitive method for probing changes in the local electronic environment that occur as the result of protein-protein interactions. To probe the potential direct interac-

tion between HSPC038 and ICln 1–159, we mixed labeled ^{15}N ICln 1–159, with an excess of unlabeled HSPC038 and followed ^{1}H and ^{15}N chemical shift perturbations in ^{1}H-^{15}N HSQC spectra (Fig. 9*d*). By comparing spectra of free and complexed ICln 1–159, it is obvious that a number of residues show small but significant chemical shift changes (Fig. 9*e*). Strikingly, when displayed on the structure of ICln (32), most of these residues (highlighted in *red* in Fig. 9*f*) face one side of the molecule, suggesting a binding interface with HSPC038 centered on two loops connecting β-strand 2 with 3 and β-strand 4 with 5. In addition, also Ala-126 and Ala-132 (both located in the α-helix; Fig. 9*f*) and Glu-138, and Gly-147 (both located outside the folded core of the protein; Fig. 9*e*) do show chemical sift changes upon complex formation. These findings fully support the results of affinity chromatography experiments indicating that the region 135–159 is important in stabilizing the ICln-HSPC038 complex. We also performed a similar experiment in the reverse direction where ^{15}N-labeled HSPC038 was mixed with unlabeled ICln 1–159. As before, small but significant chemical shift perturbations upon complex formation (Fig. 9, *a* and *b*) were observed. The residues displaying the largest perturbations (highlighted in *red* in Fig. 9*c*) were centered on the N-terminal part of the zinc finger motif, suggesting that this face of the molecule is interacting with ICln 1–159. A few residues C-terminal to the zinc finger motif also showed chemical shift perturbations; these residues were not displayed on the homology model (which is restricted to the zinc finger motif). The magnitude of the chemical shift perturbations in both experiments were smaller than what would be expected for a stoichiometric high affinity protein-protein complex. This indicates that the dissociation constant between the proteins is larger than the millimolar concentrations used in the experiments.

FIGURE 9. **Structural mapping of the HSPC038-ICln 1–159 interaction interfaces.** *a*, overlay of ^{1}H-^{15}N HSQC NMR spectra of free HSPC038 (*blue contours*) and the HSPC038-ICln 1159 complex (*red contours*). *b*, absolute difference in resonance frequency (Equation 1) between free HSPC038 and the HSPC038-ICln 1–159 complex displayed against the primary sequence. Secondary structure elements are indicated in *blue* (*β*-strands) and in *red* (*α*-helix). *c*, HSPC038 residues with a frequency difference exceeding 9 Hz (*dotted line* in *b*) upon complex formation with ICln 1–159 are colored in *red* on the HSPC038 homology model. The zinc coordinating cysteine and histidine residues are shown as *blue sticks*. *d*, overlay of ^{1}H-^{15}N HSQC NMR spectra of free ICln 1–159 (*blue contours*) and the ICln 1–159-HSPC038 complex (*red contours*). *e*, absolute difference in resonance frequency (Equation 1) between free ICln 1–159 and the ICln 1–159-HSPC038 complex displayed against the primary sequence. Secondary structure elements are indicated in *blue* (*β*-strands) and in *red* (*α*-helix). *f*, ICln 1–159 residues with a frequency difference exceeding 10 Hz (*dotted line* in *e*) upon complex formation with HSPC038 are colored in *red* on conformer number one in Protein Data Bank code 1ZYI. Secondary structure elements defined previously (32) are indicated on the structure.

DISCUSSION

HSPC038 was first identified in CD34+ hematopoietic stem progenitor cells (HSPC) (43) and shown to be a differentially expressed gene in leukocytes. Its physiological role(s) are still poorly defined. We have shown in earlier studies that the *C. elegans* homologs for ICln and HSPC038, *i.e.* IClnN2 (*icln-1*; *CO1F6.8b*) and Nx (*CO1F6.9*), functionally interact (5), and that human ICln and HSPC038 bind to each other (29). Interaction of HSPC038 with ICln suggests a role in cell volume regulation. Indeed, overexpression of HSPC038 (Fig. 2) or ICln (Fig. 1) in human cells by transient transfection markedly up-regulates ICl$_{swell}$. Similarly, knockdown of HSPC038 (Fig. 8) or ICln (6, 11) significantly reduces ICl$_{swell}$ activation. Moreover, the presence of purified ICln and/or purified HSPC038 in the intracellular solution during whole cell patch clamp recordings (Figs. 3 and 4) leads, as expected, to an up-regulation of ICl$_{swell}$. These last observations indicate that the effects of ICln or HSPC038 may not require the effect of second messengers or intracellular components that may undergo dialysis after establishment of the whole cell configuration. These experiments do

not confirm whether a molecular interaction between HSPC038 and ICln occurs or whether the two proteins act by independent mechanisms leading to the same effect. For this reason, the molecular interaction between HSPC038 and ICln was verified and demonstrated *in vitro*, as shown by native PAGE, affinity chromatography (Fig. 5 and supplemental Fig. S1) and NMR (Fig. 9) experiments. FRET experiments showed that after hypotonic shock, HSPC038 travels to the cell membrane (Fig. 6, *a* and *b*); moreover, the spatial distance between HSCP038 and ICln decreases (Fig. 6, *c* and *d*). This latter result can be explained by a molecular interaction between HSCP038 and ICln or between the two proteins and a common structure, *i.e.* another molecular partner or the cell membrane. Knowing that a similar behavior (translocation to the cell membrane) is well demonstrated for ICln (12–16) and that it is associated with ICl$_{swell}$ activation (15, 44), we hypothesized that HSPC038 could promote ICl$_{swell}$ activation by facilitating the transposition of ICln to the cell membrane. Accordingly, Western blot experiments show that ICln abundance at the membrane level is increased in HSPC038-overex-

pressing cells (supplemental Fig. S2). We exclude the possibility that HSPC038 mediates its effect on ICl$_{swell}$ and ICln abundance at the plasma membrane by increasing ICln protein expression because HSPC038 overexpression did not modify the total amount of ICln (supplemental Fig. S3). Patch clamp experiments using purified HSPC038 in the intracellular solution also excluded this hypothesis (Figs. 3 and 4).

As already reported by Ritter *et al.* (15), ICln transposes to the cell membrane after hypotonic shock; here we demonstrate for the first time that HSPC038 shows a similar behavior (Fig. 6, *a* and *b*). Although already existing under isotonicity (29), the ICln/HSPC038 interaction increases following hypotonic shock (Fig. 6, *c* and *d*). We hypothesize that HSPC038 promotes ICl$_{swell}$ activation, thereby promoting the localization of ICln to the membrane. Accordingly, Western blot data (supplemental Fig. S2) show that, following hypotonic shock, HSPC038 increases the membrane abundance of ICln. HSPC038 does not disassociate from ICln after reaching the membrane (the FRET signal does not decrease within 30 min after hypotonic shock; Fig. 6*b*). Indeed, HSPC038 remains associated with ICln (Fig. 6*d*) at the cell membrane (Fig. 6*b*), at least in the time frame explored in these experiments.

Moreover, patch clamp experiments designed to measure ICl$_{swell}$ activation in cells cotransfected with HSPC038 and ICln fused with epitopes suitable for inducing protein dimerization (Fig. 7) confirmed that the formation of an HSPC038-ICln complex improves ICl$_{swell}$ activation. The evidence that the activation of ICl$_{swell}$ is related to the ICln transposition to the cell membrane is reported elsewhere (15). Accordingly, when ICln transposition to the cell membrane is impaired, ICl$_{swell}$ activation is reduced (45).

As previously reported (29), the interaction between ICln and HSPC038 already exists in isotonic conditions; however, following hypotonic stress the interaction increases (Fig. 6*b*), ICln translocates to the cell membrane (supplemental Fig. S2), and ICl$_{swell}$ is activated (Fig. 1). Accordingly, there is no current activation in hypertonic conditions despite the HSPC038 overexpression (Fig. 2) or induced dimerization by incubation with the rapalog (Fig. 7). We conclude that the HSPC038/ICln interaction is necessary but not *per se* sufficient for the activation of ICl$_{swell}$.

By using NMR we were able to (i) reveal the structure of HSPC038 and (ii) show that both proteins (ICln and HSPC038) indeed interact on a molecular level, fully supporting the results we obtained in native PAGE experiments and by affinity chromatography (Fig. 5 and supplemental Fig. S1). The interaction between ICln and HSPC038 occurs under isotonicity (29) and increases under hypotonicity *in vivo*. In intact cells, we assume that a mechanism of volume sensing, not yet identified (46), triggers the homeostatic response of volume regulation after cell swelling, promoting, and regulating, among other processes, the increase of HSPC038/ICln interaction and ICln translocation to the cell membrane. We assume that the HSPC038/ICln interaction occurs *in vitro* as well (as shown by native PAGE, Fig. 5; affinity chromatography, Fig. 5 and supplemental Fig. S1; and NMR, Fig. 9), because both proteins are purified and are present at high concentration. This would

reveal an interaction also in the absence of any regulatory mechanism.

The NMR experiments further suggest that the interacting site on HSPC038 is centered on the N-terminal part of the zinc finger motif (Fig. 9, *a–c*). The corresponding binding site on the ICln protein was allocated on one side of the molecule, centered on two loops connecting β-strand 2 with 3 and β-strand 4 with 5 (Fig. 9, *d–f*), with the amino acids 135–159 having a role in stabilizing the complex (supplemental Fig. S1). We conclude that HSPC038 is important for the regulation of regulatory volume decrease and furthermore that HSPC038 may act as an escort, facilitating the transposition of ICln to the cell membrane following hypotonic shock and therefore facilitating the activation of ICl$_{swell}$.

REFERENCES

1. Paulmichl, M., Li, Y., Wickman, K., Ackerman, M., Peralta, E., and Clapham, D. (1992) *Nature* **356,** 238–241
2. Fürst, J., Gschwentner, M., Ritter, M., Bottà, G., Jakab, M., Mayer, M., Garavaglia, L., Bazzini, C., Rodighiero, S., Meyer, G., Eichmüller, S., Wöll, E., and Paulmichl, M. (2002) *Pflugers Arch.* **444,** 1–25
3. Gschwentner, M., Fürst, J., Ritter, M., Bazzini, C., Wöll, E., Dienstl, A., Jakab, M., König, M., Scandella, E., Rudzki, J., Botta, G., Meyer, G., Lang, F., Deetjen, P., and Paulmichl, M. (1999) *Exp. Physiol.* **84,** 1023–1031
4. Gschwentner, M., Susanna, A., Schmarda, A., Laich, A., Nagl, U. O., Ellemunter, H., Deetjen, P., Frick, J., and Paulmichl, M. (1996) *J. Allergy Clin. Immunol.* **98,** S98–S106
5. Fürst, J., Ritter, M., Rudzki, J., Danzl, J., Gschwentner, M., Scandella, E., Jakab, M., König, M., Oehl, B., Lang, F., Deetjen, P., and Paulmichl, M. (2002) *J. Biol. Chem.* **277,** 4435–4445
6. Hubert, M. D., Levitan, I., Hoffman, M. M., Zraggen, M., Hofreiter, M. E., and Garber, S. S. (2000) *Biochim. Biophys. Acta* **1466,** 105–114
7. Okada, Y., Sato, K., and Numata, T. (2009) *J. Physiol.* **587,** 2141–2149
8. Jakab, M., Fürst, J., Gschwentner, M., Bottà, G., Garavaglia, M. L., Bazzini, C., Rodighiero, S., Meyer, G., Eichmueller, S., Wöll, E., Chwatal, S., Ritter, M., and Paulmichl, M. (2002) *Cell Physiol. Biochem.* **12,** 235–258
9. Krapivinsky, G. B., Ackerman, M. J., Gordon, E. A., Krapivinsky, L. D., and Clapham, D. E. (1994) *Cell* **76,** 439–448
10. Chen, L., Wang, L., and Jacob, T. J. (1999) *Am. J. Physiol.* **276,** C182–C192
11. Gschwentner, M., Nagl, U. O., Wöll, E., Schmarda, A., Ritter, M., and Paulmichl, M. (1995) *Pflügers Arch.* **430,** 464–470
12. Meyer, G., Rodighiero, S., Guizzardi, F., Bazzini, C., Bottà, G., Bertocchi, C., Garavaglia, L., Dossena, S., Manfredi, R., Sironi, C., Catania, A., and Paulmichl, M. (2004) *FEBS Lett.* **559,** 45–50
13. Musch, M. W., Davis-Amaral, E. M., Vandenburgh, H. H., and Goldstein, L. (1998) *Pflügers Arch.* **436,** 415–422
14. Musch, M. W., Luer, C. A., Davis-Amaral, E. M., and Goldstein, L. (1997) *J. Exp. Zool.* **277,** 460–463
15. Ritter, M., Ravasio, A., Jakab, M., Chwatal, S., Fürst, J., Laich, A., Gschwentner, M., Signorelli, S., Burtscher, C., Eichmüller, S., and Paulmichl, M. (2003) *J. Biol. Chem.* **278,** 50163–50174
16. Tamma, G., Procino, G., Strafino, A., Bononi, E., Meyer, G., Paulmichl, M., Formoso, V., Svelto, M., and Valenti, G. (2007) *Endocrinology* **148,** 1118–1130
17. Okada, Y. (1997) *Am. J. Physiol.* **273,** C755–C789
18. Strange, K. (1998) *J. Gen. Physiol.* **111,** 617–622
19. Fürst, J., Bazzini, C., Jakab, M., Meyer, G., König, M., Gschwentner, M., Ritter, M., Schmarda, A., Bottà, G., Benz, R., Deetjen, P., and Paulmichl, M. (2000) *Pflügers Arch.* **440,** 100–115
20. Garavaglia, M., Dopinto, S., Ritter, M., Fürst, J., Saino, S., Guizzardi, F., Jakab, M., Bazzini, C., Vezzoli, V., Dossena, S., Rodighiero, S., Sironi, C., Bottà, G., Meyer, G., Henderson, R. M., and Paulmichl, M. (2004) *Cell Physiol. Biochem.* **14,** 231–240
21. Garavaglia, M. L., Rodighiero, S., Bertocchi, C., Manfredi, R., Fürst, J., Gschwentner, M., Ritter, M., Bazzini, C., Bottà, G., Jakab, M., Meyer, G.,

and Paulmichl, M. (2002) *Pflugers Arch.* **443,** 748–753

22. Li, C., Breton, S., Morrison, R., Cannon, C. L., Emma, F., Sanchez-Olea, R., Bear, C., and Strange, K. (1998) *J. Gen. Physiol.* **112,** 727–736

23. Krapivinsky, G., Pu, W., Wickman, K., Krapivinsky, L., and Clapham, D. E. (1998) *J. Biol. Chem.* **273,** 10811–10814

24. Larkin, D., Murphy, D., Reilly, D. F., Cahill, M., Sattler, E., Harriott, P., Cahill, D. J., and Moran, N. (2004) *J. Biol. Chem.* **279,** 27286–27293

25. Li, S., Armstrong, C. M., Bertin, N., Ge, H., Milstein, S., Boxem, M., Vidalain, P. O., Han, J. D., Chesneau, A., Hao, T., Goldberg, D. S., Li, N., Martinez, M., Rual, J. F., Lamesch, P., Xu, L., Tewari, M., Wong, S. L., Zhang, L. V., Berriz, G. F., Jacotot, L., Vaglio, P., Reboul, J., Hirozane-Kishikawa, T., Li, Q., Gabel, H. W., Elewa, A., Baumgartner, B., Rose, D. J., Yu, H., Bosak, S., Sequerra, R., Fraser, A., Mango, S. E., Saxton, W. M., Strome, S., Van Den Heuvel, S., Piano, F., Vandenhaute, J., Sardet, C., Gerstein, M., Doucette-Stamm, L., Gunsalus, K. C., Harper, J. W., Cusick, M. E., Roth, F. P., Hill, D. E., and Vidal, M. (2004) *Science* **303,** 540–543

26. Jakab, M., and Ritter, M. (2006) *Contrib. Nephrol.* **152,** 161–180

27. Pu, W. T., Krapivinsky, G. B., Krapivinsky, L., and Clapham, D. E. (1999) *Mol. Cell Biol.* **19,** 4113–4120

28. Fürst, J., Bottà, G., Saino, S., Dopinto, S., Gandini, R., Dossena, S., Vezzoli, V., Rodighiero, S., Bazzini, C., Garavaglia, M. L., Meyer, G., Jakab, M., Ritter, M., Wappl-Kornherr, E., and Paulmichl, M. (2006) *Acta Physiol.* **187,** 43–49

29. Eichmüller, S., Vezzoli, V., Bazzini, C., Ritter, M., Fürst, J., Jakab, M., Ravasio, A., Chwatal, S., Dossena, S., Bottà, G., Meyer, G., Maier, B., Valenti, G., Lang, F., and Paulmichl, M. (2004) *J. Biol. Chem.* **279,** 7136–7146

30. Blumenthal, T., Evans, D., Link, C. D., Guffanti, A., Lawson, D., Thierry-Mieg, J., Thierry-Mieg, D., Chiu, W. L., Duke, K., Kiraly, M., and Kim, S. K. (2002) *Nature* **417,** 851–854

31. Morgan, R. A., Couture, L., Elroy-Stein, O., Ragheb, J., Moss, B., and Anderson, W. F. (1992) *Nucleic Acids Res.* **20,** 1293–1299

32. Fürst, J., Schedlbauer, A., Gandini, R., Garavaglia, M. L., Saino, S., Gschwentner, M., Sarg, B., Lindner, H., Jakab, M., Ritter, M., Bazzini, C., Botta, G., Meyer, G., Kontaxis, G., Tilly, B. C., Konrat, R., and Paulmichl, M.

33. Chen, B. P., and Hai, T. (1994) *Gene* **139,** 73–75

34. Delaglio, F., Grzesiek, S., Vuister, G. W., Zhu, G., Pfeifer, J., and Bax, A. (1995) *J. Biomol. NMR* **6,** 277–293

35. Helgstrand, M., Kraulis, P., Allard, P., and Härd, T. (2000) *J. Biomol. NMR* **18,** 329–336

36. Schedlbauer, A., Kontaxis, G., König, M., Fürst, J., Jakab, M., Ritter, M., Garavaglia, L., Bottà, G., Meyer, G., Paulmichl, M., and Konrat, R. (2003) *J. Biomol. NMR* **27,** 399–400

37. Kiefer, F., Arnold, K., Künzli, M., Bordoli, L., and Schwede, T. (2009) *Nucleic Acids Res.* **37,** D387–D392

38. Arnold, K., Bordoli, L., Kopp, J., and Schwede, T. (2006) *Bioinformatics* **22,** 195–201

39. Ho, S. N., Biggar, S. R., Spencer, D. M., Schreiber, S. L., and Crabtree, G. R. (1996) *Nature* **382,** 822–826

40. Choi, J., Chen, J., Schreiber, S. L., and Clardy, J. (1996) *Science* **273,** 239–242

41. Gschwentner, M., Susanna, A., Wöll, E., Ritter, M., Nagl, U. O., Schmarda, A., Laich, A., Pinggera, G. M., Ellemunter, H., Huemer, H., Deetjen, P., and Paulmichl, M. (1995) *Mol. Med.* **1,** 407–417

42. Wienk, H., Lammers, I., Hotze, A., Wu, J., Wechselberger, R. W., Owens, R., Stammers, D. K., Stuart, D., Kaptein, R., and Folkers, G. E. (2009) *Biochemistry* **48,** 4431–4439

43. Zhang, Q. H., Ye, M., Wu, X. Y., Ren, S. X., Zhao, M., Zhao, C. J., Fu, G., Shen, Y., Fan, H. Y., Lu, G., Zhong, M., Xu, X. R., Han, Z. G., Zhang, J. W., Tao, J., Huang, Q. H., Zhou, J., Hu, G. X., Gu, J., Chen, S. J., and Chen, Z. (2000) *Genome Res.* **10,** 1546–1560

44. Jakab, M., Grundbichler, M., Benicky, J., Ravasio, A., Chwatal, S., Schmidt, S., Strbak, V., Fürst, J., Paulmichl, M., and Ritter, M. (2006) *Cell Physiol Biochem.* **18,** 21–34

45. Gandini, R., Dossena, S., Vezzoli, V., Tamplenizza, M., Salvioni, E., Ritter, M., Paulmichl, M., and Furst, J. (2008) *Cell Physiol Biochem.* **22,** 579–590

46. Hoffmann, E. K., and Simonsen, L. O. (1989) *Physiol. Rev.* **69,** 315–382